A Microscopic Optical Potential Approach to ^{6,8}He+p Elastic Scattering

V.K. Lukyanov[1], E.V. Zemlyanaya[1], K.V. Lukyanov[1], D.N. Kadrev[2], A.N. Antonov[2], M.K. Gaidarov[2], S.E. Massen[3]

[1]Joint Institute for Nuclear Research, Dubna 141980, Russia
[2]Institute for Nuclear Research and Nuclear Energy, Bulgarian Academy of Sciences, Sofia 1784, Bulgaria
[3]Department of Theoretical Physics, Aristotle University of Thessaloniki, 54124 Thessaloniki, Greece

28th International Workshop on Nuclear Theory
June 22-27, 2009
Rila Mountains, Bulgaria

Introduction

Structure of exotic nuclei ⇒ analyses of their elastic scattering on protons or light targets at different energies

^{6}He: 25.2, 38.3, 41.6 and 71 MeV/N

^{8}He: 15.7, 25.2, 32, 66 and 73 MeV/N

He and **Li** isotopes**:** 700 MeV/N

Phenomenological and microscopic methods:

- Coordinate-space *g*-matrix folding method
- ReOP is microscopically calculated using the folding approach, while the ImOP and the SO terms have been determined phenomenologically

The main aim: to calculate *$d\sigma/d\Omega$* of elastic ^{6,8}He+p scattering at energies less than 100 MeV/N studying the possibility to describe the existing experimental data by calculating microscopically not only the ReOP (in a double folding procedure) but also the ImOP (instead of using phenomenological one) within the high-energy approximation (HEA) and using a minimal number of fitting parameters.

What we study:

- the limits of applicability of the HEA OP for different regions of angles ant incident energies
- the sensitivity of the cross sections to the nuclear densities of ^{6}He and ^{8}He
- the role of the SO interaction and the non-linearity in the calculations of the OP's
- the nuclear surface effects
- the role of the renormalization of the depths of ReOP and ImOP
- the possibility to involve additional physical criteria for a better description of limited number of experimental data

Basic Ingredients of the Cross Sections Calculations

Optical potential (OP):

$$U_{opt}(r) = N_R V^F(r) + i N_I W^H(r) + \\ + 2\lambda_\pi^2 \left\{ N_R^{SO} V_0^F \frac{1}{r}\frac{df_R(r)}{dr} + i N_I^{SO} W_0^H \frac{1}{r}\frac{df_I(r)}{dr} \right\} (\mathbf{l}.\mathbf{s}) \quad (1)$$

1. Direct and exchange parts of the real OP (ReOP)

$$V^F(r) = V^D(r) + V^{EX}(r) \quad (2)$$

$$V_{IS}^D(r) = \int \rho_2(\mathbf{r}_2) g(E) F(\rho_2) v_{00}^D(s) d\mathbf{r_2} \quad (3)$$

$$V_{IV}^D(r) = \int \delta\rho_2(\mathbf{r}_2) g(E) F(\rho_2) v_{01}^D(s) d\mathbf{r_2} \quad (4)$$

$$\rho_2(\mathbf{r}_2) = \rho_{2,p}(\mathbf{r}_{2,p}) + \rho_{2,n}(\mathbf{r}_{2,n}) \tag{5}$$

$$\delta\rho_2(\mathbf{r}_2) = \rho_{2,p}(\mathbf{r}_{2,p}) - \rho_{2,n}(\mathbf{r}_{2,n}) \tag{6}$$

$$g(E) = 1 - 0.003E \tag{7}$$

For the NN potentials v_{00}^D and v_{01}^D we use the expression for the CDM3Y6-type of the effective interaction based on the solution of the equation for the g-matrix, in which the Paris NN potential has been used.

$$F(\rho) = C\left[1 + \alpha e^{-\beta\rho(\mathbf{r})} - \gamma\rho(\mathbf{r})\right], \tag{8}$$

where C=0.2658, α=3.8033, β=1.4099 fm^3, and γ=4.0 fm^3.

$$\begin{aligned} V_{IS}^{EX}(r) &= g(E)\int \rho_2(\mathbf{r}_2, \mathbf{r}_2 - \mathbf{s})F\left[\rho_2\left(\mathbf{r}_2 - \frac{\mathbf{s}}{2}\right)\right] \\ &\times v_{00}^{EX}(s)j_0[k(r)s]d\mathbf{r}_2 \end{aligned} \tag{9}$$

$$\rho_2\left(\mathbf{r}_2, \mathbf{r}_2 - \mathbf{s}\right) \;\simeq\; \rho_2\left(\left|\mathbf{r}_2 - \frac{\mathbf{s}}{2}\right|\right) \hat{j}_1\left[k_{F,2}\left(\left|\mathbf{r}_2 - \frac{\mathbf{s}}{2}\right|\right) \cdot s\right] \tag{10}$$

with

$$\hat{j}_1(x) = \frac{3}{x} j_1(x) = \frac{3}{x^3}(\sin x - x\cos x) \tag{11}$$

$$k^2(r) = \left(\frac{2m}{\hbar^2}\right) \left[E_{c.m.} - V_c(r) - V(r)\right] \left(\frac{1 + A_2}{A_2}\right) \tag{12}$$

$$k_{F,2}(r) = \left\{ \frac{5}{3\rho} \left[\tau(\rho) - \frac{1}{4} \nabla^2 \rho(r) \right] \right\}^{1/2} \tag{13}$$

$$\begin{aligned} \frac{\tau(\rho)}{2} \;&\simeq\; \tau_q(\rho_q) = \frac{3}{5}\left(3\pi^2\right)^{2/3} \left[\rho_q(r)\right]^{5/3} \\ &+\; \frac{\left|\nabla \rho_q(r)\right|^2}{36 \rho_q(r)} + \frac{\nabla^2 \rho_q(r)}{3} \end{aligned} \tag{14}$$

2. OP within the high-energy approximation

$$U_{opt}^{H} = V^{H} + iW^{H} = -\frac{\hbar v}{(2\pi)^2}(\bar{\alpha}_{NN} + i)\bar{\sigma}_{NN} \times \int_0^\infty dq q^2 j_0(qr)\rho_2(q) f_{NN}(q) \quad (15)$$

3. Spin-orbit term

$$V_{LS}(r) = 2\lambda_\pi^2 \left[V(0)\frac{1}{r}\frac{df(r_R)}{dr} + W(0)\frac{1}{r}\frac{df(r_I)}{dr} \right] (\mathbf{l}\cdot\mathbf{s}) \quad (16)$$

^{6}He+p

$$(A) \qquad U_{opt}^{A} = N_R^A V^H + i N_I^A W^H \tag{17}$$

$$(B) \qquad U_{opt}^{B} = N_R^B V^F + i N_I^B W^H \tag{18}$$

$$(C) \qquad U_{opt}^{C} = N_R^C V^F + i N_I^C V^F \tag{19}$$

^{8}He+p

$$U'_{opt}(r) = U_{opt}(r) - i4aN_S \frac{dV^F(r)}{dr} \tag{20}$$

Density distributions of ^{6}He and ^{8}He:

1. Tanihata densities

$$\rho^X_{point} = \frac{2}{\pi^{3/2}}\left\{\frac{1}{a^3}\exp\left[-\left(\frac{r}{a}\right)^2\right] + \frac{1}{b^3}\frac{(X-2)}{3}\left(\frac{r}{b}\right)^2\exp\left[-\left(\frac{r}{b}\right)^2\right]\right\}$$

$$a^2 = a^{*2}\left(1-\frac{1}{A}\right), \qquad b^2 = b^{*2}\left(1-\frac{1}{A}\right) \tag{21}$$

^{6}He: a=1.40 fm; b=2.04 fm; R^p_{rms}=1.72 fm

^{8}He: a=1.43 fm; b=1.93 fm; R^p_{rms}=1.76 fm; R^n_{rms}=2.69 fm

2. COSMA densities
3. LSSM densities
4. JCM densities: correlation factor=$1-\exp^{-\beta^2 r^2}$

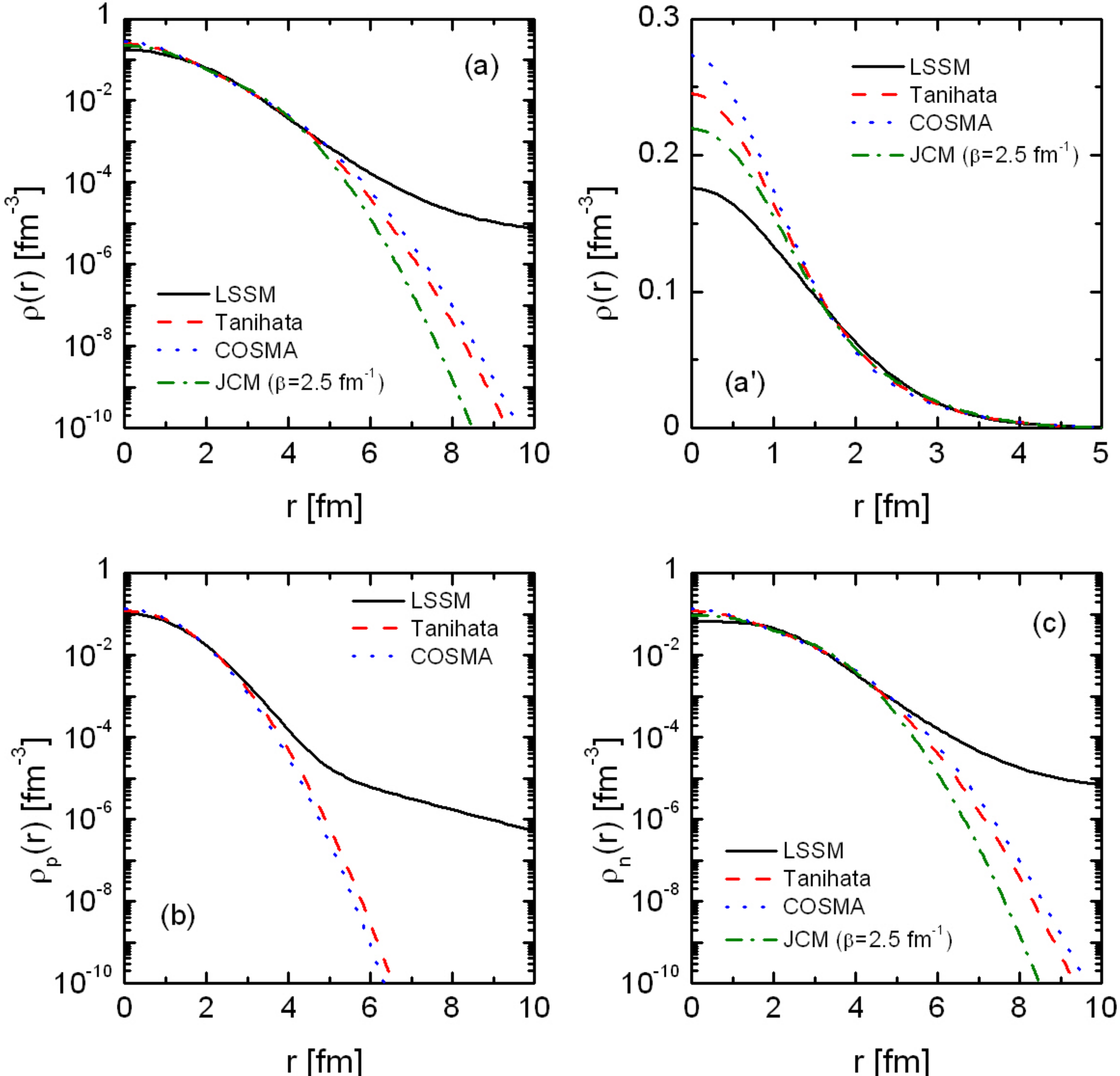

(a)
LSSM
Tanihata
COSMA
JCM (β=2.5 fm-1)
ρ(r) [fm-3]
r [fm]
(a')
LSSM
Tanihata
COSMA
JCM (β=2.5 fm-1)
ρ(r) [fm-3]
r [fm]
(b)
LSSM
Tanihata
COSMA
ρp(r) [fm-3]
r [fm]
(c)
LSSM
Tanihata
COSMA
JCM (β=2.5 fm-1)
ρn(r) [fm-3]
r [fm]

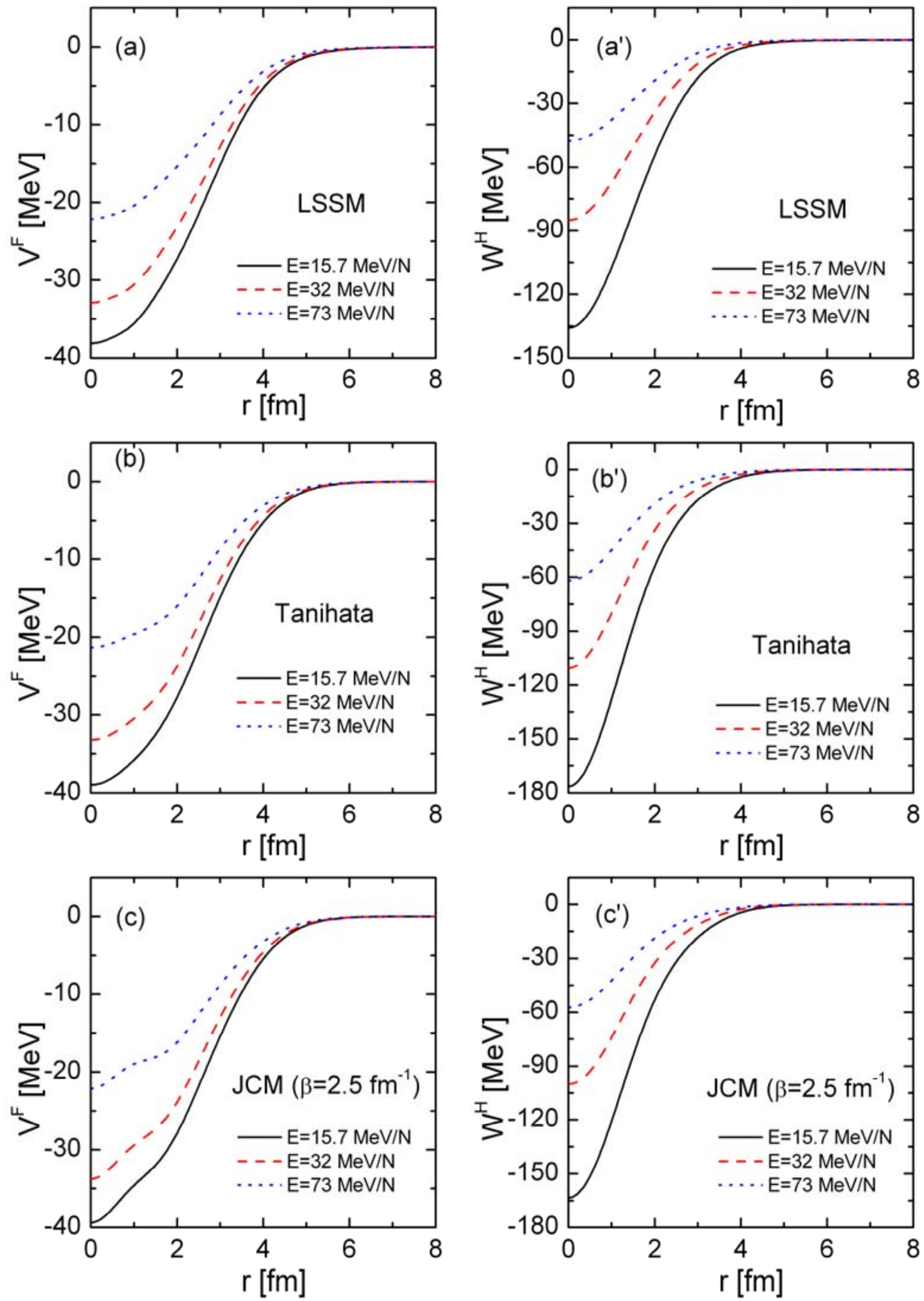

(a)
LSSM
E=15.7 MeV/N
E=32 MeV/N
E=73 MeV/N
V^F [MeV]
r [fm]
(a')
LSSM
E=15.7 MeV/N
E=32 MeV/N
E=73 MeV/N
W^H [MeV]
r [fm]
(b)
Tanihata
E=15.7 MeV/N
E=32 MeV/N
E=73 MeV/N
V^F [MeV]
r [fm]
(b')
Tanihata
E=15.7 MeV/N
E=32 MeV/N
E=73 MeV/N
W^H [MeV]
r [fm]
(c)
JCM (β=2.5 fm^{-1})
E=15.7 MeV/N
E=32 MeV/N
E=73 MeV/N
V^F [MeV]
r [fm]
(c')
JCM (β=2.5 fm^{-1})
E=15.7 MeV/N
E=32 MeV/N
E=73 MeV/N
W^H [MeV]
r [fm]

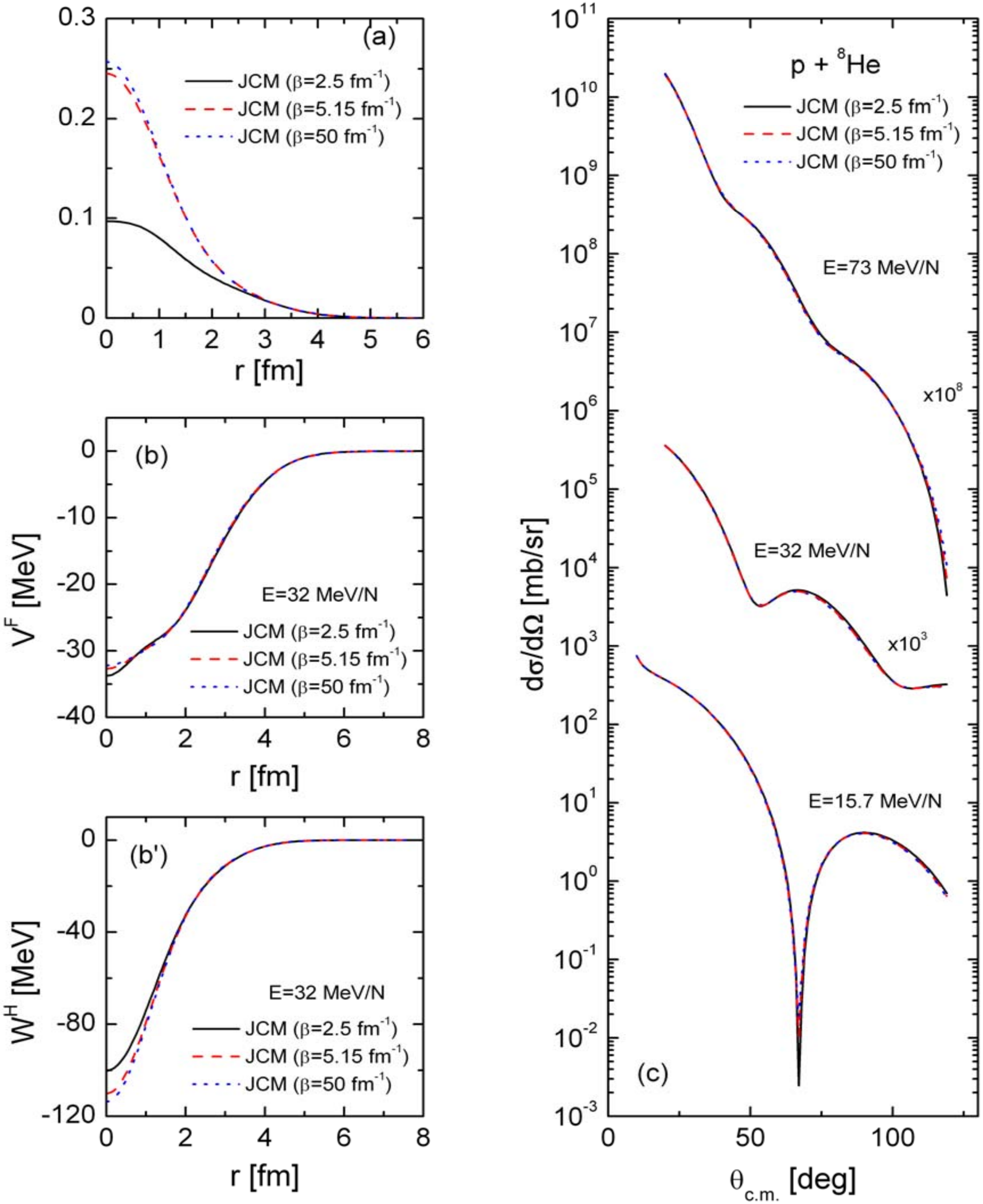

(a)
JCM (β=2.5 fm⁻¹)
JCM (β=5.15 fm⁻¹)
JCM (β=50 fm⁻¹)
r [fm]
(b)
V^F [MeV]
E=32 MeV/N
JCM (β=2.5 fm⁻¹)
JCM (β=5.15 fm⁻¹)
JCM (β=50 fm⁻¹)
r [fm]
(b')
W^H [MeV]
E=32 MeV/N
JCM (β=2.5 fm⁻¹)
JCM (β=5.15 fm⁻¹)
JCM (β=50 fm⁻¹)
r [fm]
p + ^{8}He
JCM (β=2.5 fm⁻¹)
JCM (β=5.15 fm⁻¹)
JCM (β=50 fm⁻¹)
E=73 MeV/N
x10^8
E=32 MeV/N
x10^3
E=15.7 MeV/N
(c)
dσ/dΩ [mb/sr]
$\theta_{c.m.}$ [deg]

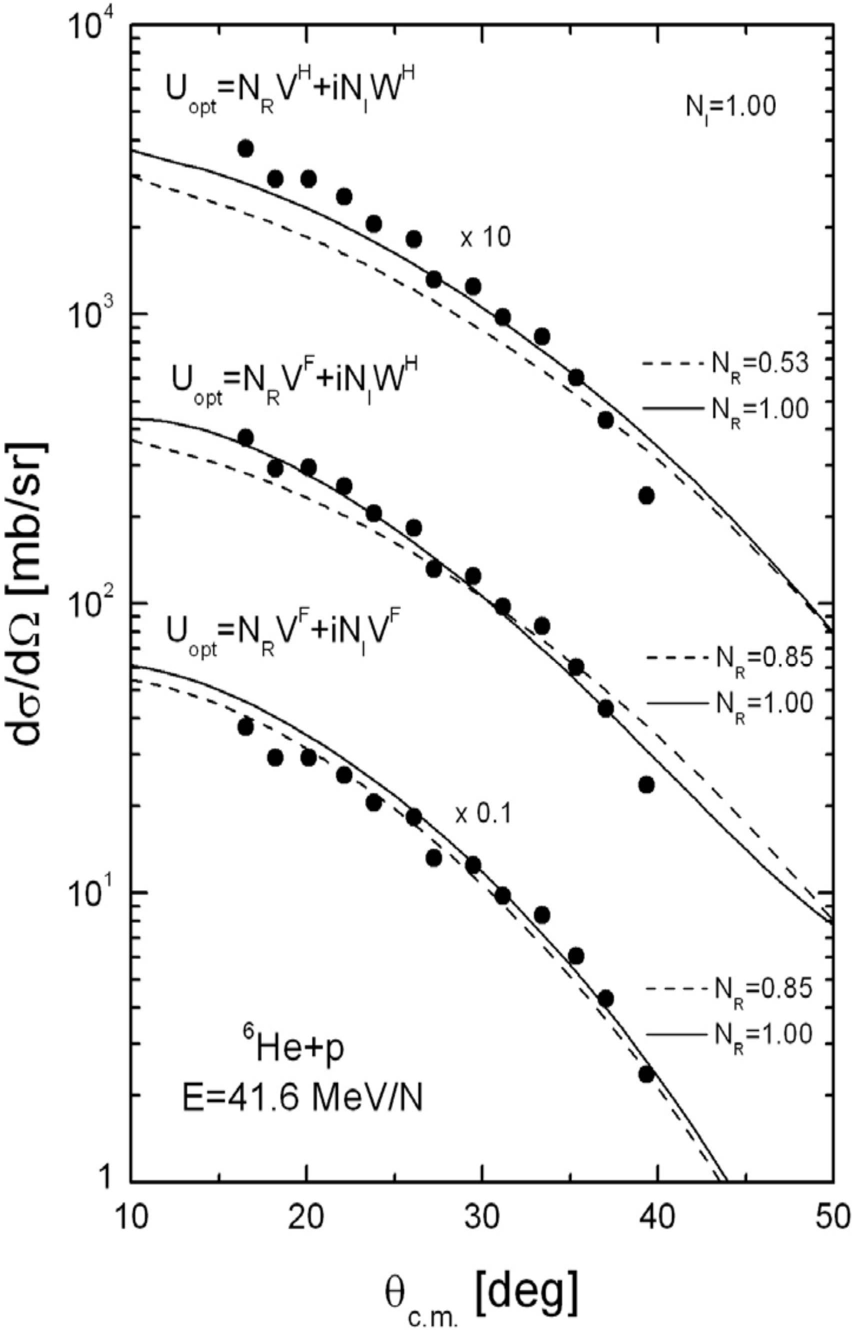

$U_{opt}=N_R V^H+iN_I W^H$
N_I=1.00
x 10
$U_{opt}=N_R V^F+iN_I W^H$
N_R=0.53
N_R=1.00
$U_{opt}=N_R V^F+iN_I V^F$
N_R=0.85
N_R=1.00
x 0.1
N_R=0.85
N_R=1.00
^{6}He+p
E=41.6 MeV/N
dσ/dΩ [mb/sr]
$\theta_{c.m.}$ [deg]

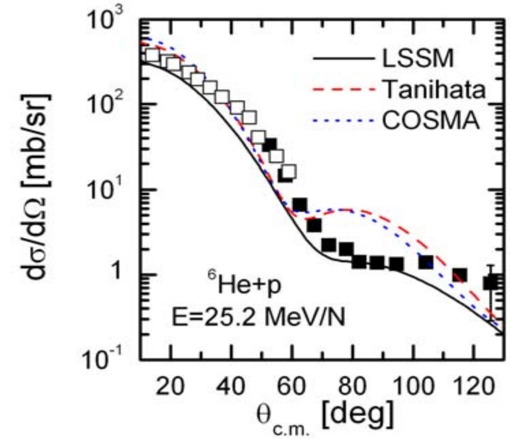

LSSM
Tanihata
COSMA
^{6}He+p
E=25.2 MeV/N
dσ/dΩ [mb/sr]
$\theta_{c.m.}$ [deg]

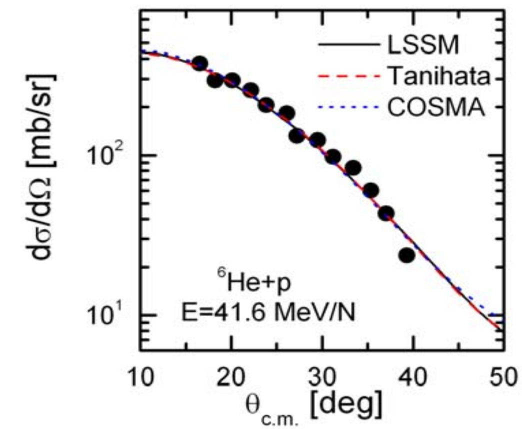

LSSM
Tanihata
COSMA
^{6}He+p
E=41.6 MeV/N
dσ/dΩ [mb/sr]
$\theta_{c.m.}$ [deg]

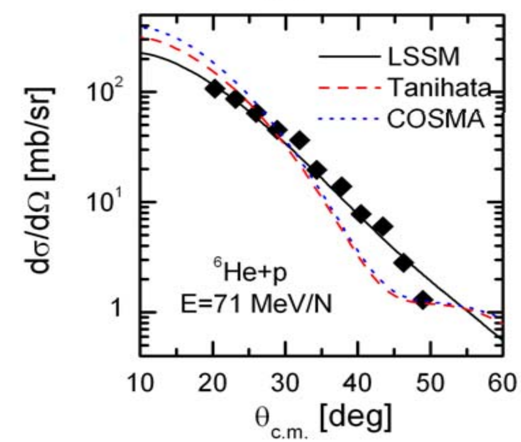

LSSM
Tanihata
COSMA
^{6}He+p
E=71 MeV/N
dσ/dΩ [mb/sr]
$\theta_{c.m.}$ [deg]

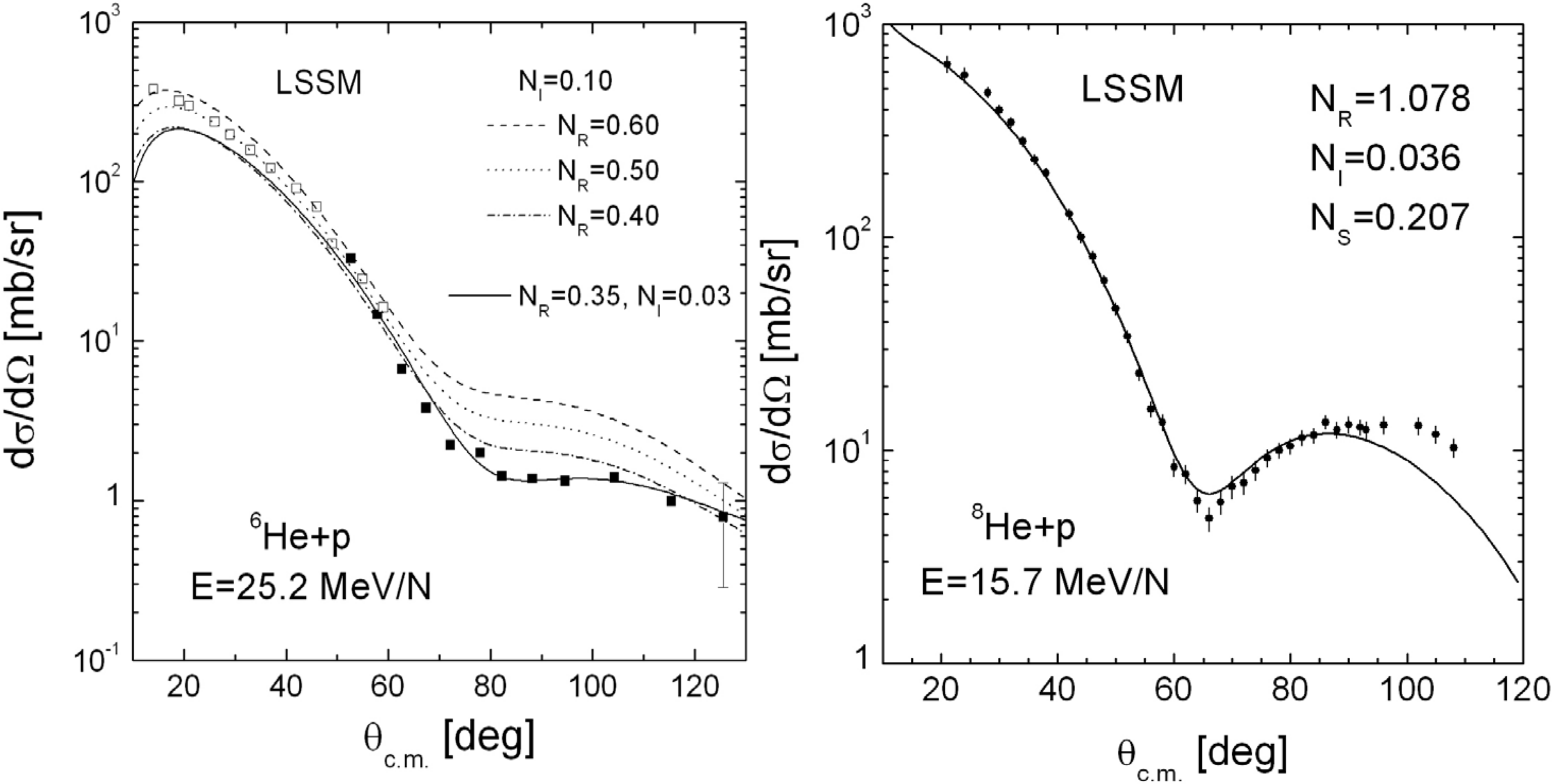

LSSM
N_I=0.10
N_R=0.60
N_R=0.50
N_R=0.40
N_R=0.35, N_I=0.03
^{6}He+p
E=25.2 MeV/N
dσ/dΩ [mb/sr]
θ c.m. [deg]
LSSM
N_R=1.078
N_I=0.036
N_S=0.207
^{8}He+p
E=15.7 MeV/N
dσ/dΩ [mb/sr]
θ c.m. [deg]

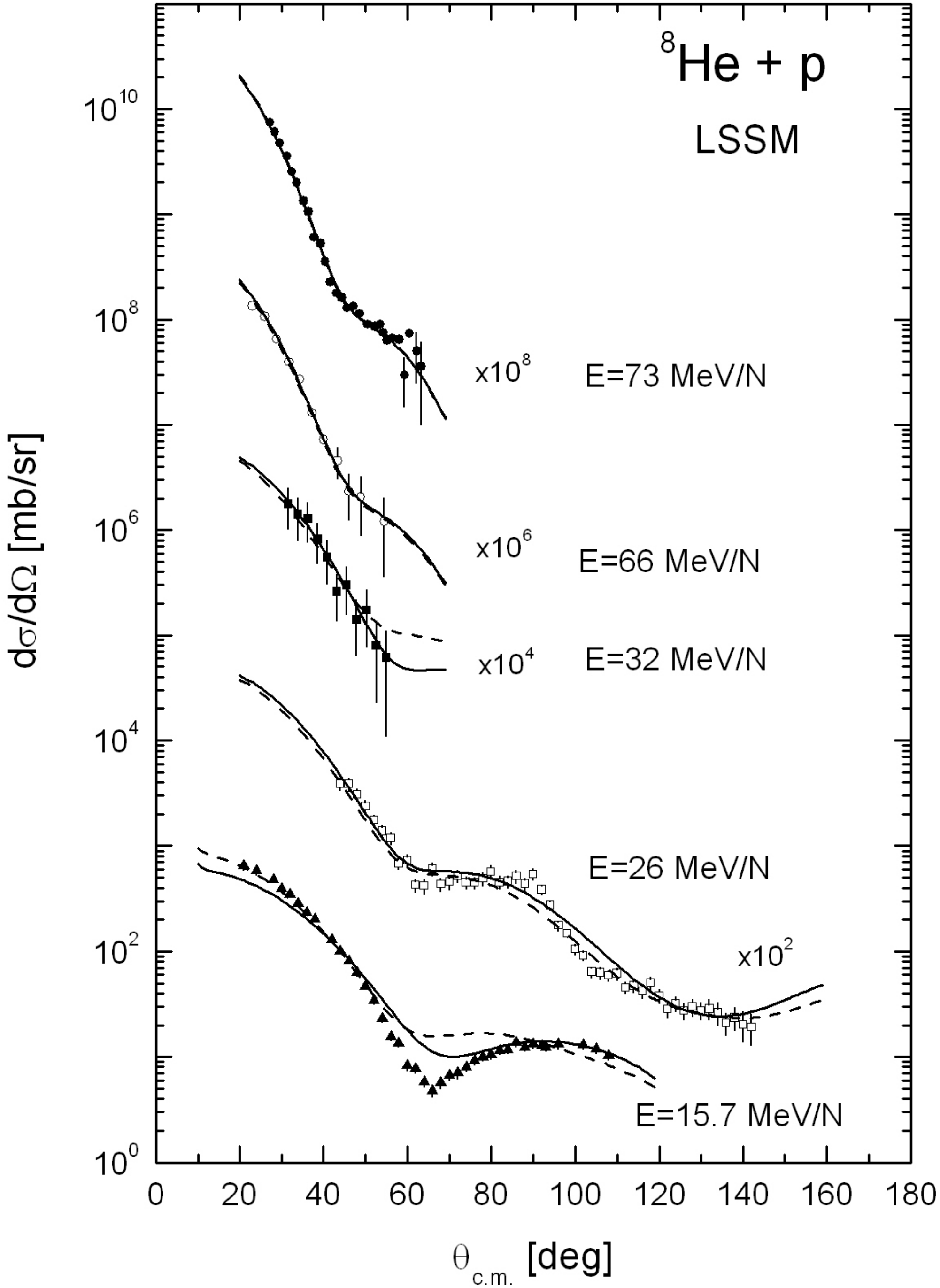

The renormalization parameters N_R, N_I, N_R^{SO} and N_I^{SO} obtained by fitting the experimental data in the case of LSSM density. The energies are in MeV/N and the total reaction cross sections σ_R are in mb.

E	N_R	N_I	N_R^{SO}	N_I^{SO}	σ_R
15.7	1.0	0.236	0	0	603.6
15.7	0.9	0.1	0.107	0.040	693
26	0.422	0.104	0.090	0.010	275.11
26	0.439	0.144	0.087	0.023	377.22
32	0.438	0.036	0.096	0	71.9
32	1.0	0.374	0	0	419.5
66	0.876	0.071	0	0	55.7
66	0.854	0.086	0	0	65.9
73	0.875	0.02	0	0	1.48
73	0.869	0.01	0.010	0.002	1.22

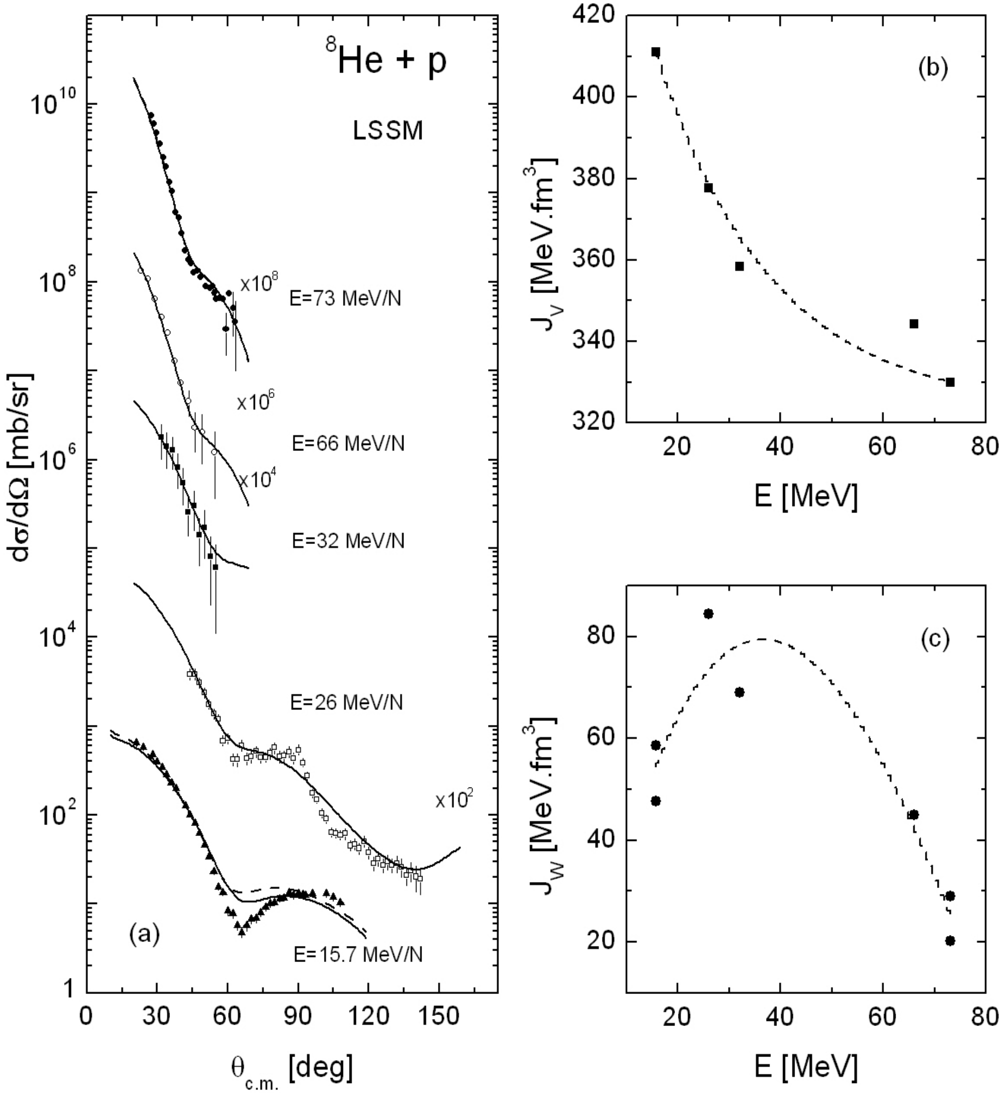

$$J_V = (4\pi/A) \int dr\, r^2 \left[N_R V^F(r) \right]$$

$$J_W = (4\pi/A) \int dr\, r^2 \left[N_I W^H(r) \right]$$

The parameters N_R, N_I, N_R^{SO} and N_R^{SO}, the volume integrals J_V and J_W (in MeV.fm^3) as functions of the energy E (in MeV/N) and the total reaction cross sections σ_R (in mb) for the ^{8}He+p scattering in the case of LSSM density.

E	N_R	N_I	N_R^{SO}	N_I^{SO}	J_V	J_W	σ_R
15.7	0.630	0.064	0.139	0.070	411.1	58.6	722.0
15.7	0.630	0.052	0.166	0.057	411.1	47.6	701.2
26	0.644	0.128	0.035	0.026	377.7	84.35	381.2
32	0.648	0.120	0.062	0.022	358.3	69	302.7
66	0.852	0.131	0	0	344.2	45	95.2
73	0.869	0.090	0.004	0	330.0	29	60.9
73	0.869	0.063	0.010	0	330.0	20.25	43.9

Conclusions

1. The optical potentials and cross sections of ^{6}He+p (E=25.2,41.6 and 71 MeV/N) and ^{8}He+p (E=15.7,26.25, 32, 66 and 73 MeV/N) elastic scattering were calculated and comparison with the available experimental data was performed.

- The ReOP (V^F) was calculated microscopically using the folding procedure and M3Y effective interaction based on the Paris NN potential.
- The ImOP (W^H) was calculated within the HEA.
- Different model densities of protons and neutrons in ^{6}He and ^{8}He were used in the calculations: Tanihata, COSMA, LSSM and JCM.
- Three different combinations of V^F, V^H and and W^H were used for the OP in calculations of the elastic ^{6}He+p cross sections.
- The SO contribution to the OP was included in the calculations.
- The cross sections were calculated by numerical integration of the Schrödinger equation by means of the DWUCK4 code using all interactions obtained (Coulomb plus nuclear optical potential).

2. The results show that the LSSM densities of ^{6}He and ^{8}He which have more diffuse tails at larger *r* than the densities based on Gaussians lead to a better agreement with the data for the ^{6,8}He+p elastic scattering at different energies.

3. It was shown that, generally, at energies E>25 MeV/N a good agreement with the experimental data for the differential cross sections can be achieved using OP with calculated both V^F and W^H varying mainly the volume part of the OP neglecting SO contribution.

4. The explanation of the ^{6,8}He+p cross sections at lower energies (E<25 MeV/N) needs accounting for the effects of the nuclear surface. In this case the use of ImOP of the HEA type is limited. A more successful explanation of the cross section at low energies could be given by inclusion of polarization contributions due to virtual excitations of inelastic and decay channels of the reactions.

5. The study of the density and energy dependence of the effective M3Y NN forces shows small differences between OP's calculated with and without inclusion of the in-medium effect. The difference between the corresponding cross sections appears at larger angles and increases with the energy increase.

6. It was shown that the effects of the Jastrow central short-range NN correlations on the OP's and on the shape of differential cross sections are weak.

7. The problem of the ambiguity of the values of the parameters N_R, N_I, N_R^{SO}, and N_I^{SO} when the fitting procedure is applied to a limited number of experimental data is considered. A physical criteria imposed in our work on the choice of the values of the parameters N were the known behavior of the volume integrals J_V and J_W as functions of the incident energy in the interval $0<E_{inc}<100$ MeV/N, as well as the values of the total cross section of scattering and reaction.

This approach can be used along with other more sophisticated methods like that from the microscopic *g*-matrix description of the complex optical potential ant others.